

Dynamics of the Periodically-Forced Duffing Oscillator

Andrew Champion,¹ Ross Granowski,² Aemen Lodhi,¹ and Suchithra Ravi³

¹*School of Computer Science, Georgia Institute of Technology, Atlanta, Georgia 30332, USA*

²*School of Mathematics, Georgia Institute of Technology, Atlanta, Georgia 30332, USA*

³*School of Electrical Engineering, Georgia Institute of Technology, Atlanta, Georgia 30332, USA*

(Dated: 14 December 2012)

We investigate the behavior of a Duffing oscillator subjected to lateral periodic forcing. We analyzed experimental results and compare them to results from our simulations. We explain the impact of asymmetry in the oscillator wells and show how it can impact the emergence of chaos in the system.

I. INTRODUCTION

In this study we explore the dynamics of the Duffing oscillator[?] when subjected to periodic lateral force. Figure 1 illustrates the concept of the system. It shows a buckling beam undergoing lateral periodic force applied to one side. Two electromagnets attract the beam to one of two stable positions. This system can be modeled by the “Duffing equation” which is a non-autonomous, second-order ODE:

$$\ddot{x} + \delta\dot{x} - \alpha x + \beta x^3 = f \cos(\omega t) \quad (1)$$

We chose to study this system as it provides us with a relatively simple model to study the transitions between periodic behavior and chaos. The small number of param-

eters allows us to isolate the effect of initial conditions from small variations in the parameters. Existing literature on the subject has reported sudden transitions between periodicity and chaos. The system is simple enough that we can study its qualitative and quantitative properties by using three popular approaches of scientific inquiry: (a) constructing a physical experiment to demonstrate the behavior, (b) studying the model analytically after some simplifications and (c) using computer simulations to complement the previous two approaches.

Our objective is to analyze the bifurcations of the system in the (f, ω) plane for fixed values of α , β and δ . We focus on different ranges of f to determine the thresholds of these bifurcations. Thus, we can use this

system to demonstrate how a single parameter in a simple model can result in the onset of chaos.

The rest of this study is organized as follows. Section III discusses the model. Section IV outlines the methods we employed in this study. We provide our results in section V followed by the conclusion in section VI.

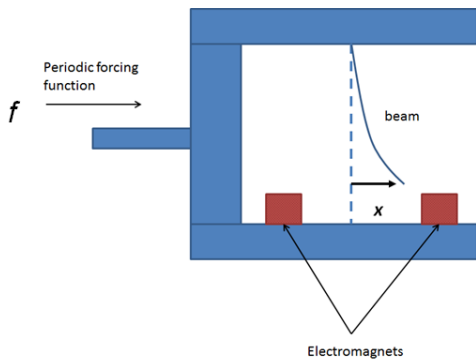


FIG. 1. Conceptual illustration of the system

II. RELATED WORK

III. MODEL

The system can be modeled by the following equation:

$$\ddot{x} + \delta\dot{x} - \alpha x + \beta x^3 = f \cos(\omega t) \quad (2)$$

In order to understand the equation we first consider the simplest case where set $\delta = 0$ and $f = 0$. The equation is reduced to:

$$\ddot{x} - \alpha x + \beta x^3 = 0 \quad (3)$$

which is a Newtonian system with potential $V(x) = \frac{\beta}{4}x^4 - \frac{\alpha}{2}x^2$. The trajectories are curves of constant energy $E(x, \dot{x}) = \frac{1}{2}\dot{x}^2 + V(x)$. It is easy to see that we have a saddle at the origin and center at $(\sqrt{\pm\frac{\alpha}{\beta}}, 0)$. Other than the two homoclinic orbits from the origin to itself and the two centers, we have that all other trajectories are in fact closed orbits.

Increasing the complexity of the simplified model, we add the dissipation term i.e., we set $\delta > 0$. In this system, heuristically, trajectories spiral into what are now stable

fixed points at $(\sqrt{\pm\frac{\alpha}{\beta}}, 0)$. In this case, the energy decreases along the trajectories of the system:

$$\frac{d}{dt}E = \dot{x}(\ddot{x} + \beta x^3 - \alpha x) = -\delta\dot{x}^2 \leq 0$$

It can be shown that, except for the stable manifolds of the saddle, all trajectories of this system tend towards one of the stable fixed points.

In order to understand the impact of the magnitude of the forcing term f we consider three ranges for its magnitude when it is greater than zero:

1. *f close to zero*: For small values of f we find that we have stable limit cycles near what were stable fixed points for $f = 0$, and almost all trajectories eventually converge to one of the two limit cycles (namely all except for the mea-

sure zero stable manifolds of the saddle point at the origin).

2. *Very large f* : it can be shown there is one globally stable limit cycle attracting all trajectories.
3. *Intermediate values of f* : For this range of values we have chaotic behavior of trajectories in phase space. This is essentially due to the fact that as we increase f from zero we eventually cause the stable and unstable manifolds of the saddle at $(0, 0)$ to intersect, and hence to intersect infinitely many times. The presence of infinitely many homoclinic intersection points in (a compact region of) phase space causes the trajectories to have very complex topological structures. We are most interested in analysis of this range of values.

IV. METHODS

A. Experimental Setup

We constructed a physical apparatus on the same lines as shown in figure 1. A schematic diagram of our apparatus is shown in figure 2. We attached a slender metallic beam to a rigid frame made from 80/20. The beam was cut from shim stock of thickness

.007 inches. Two rare earth magnets were attached symmetrically to the top of the frame. The magnets in our experimental setup had uneven strength. As a result, the metallic beam always buckled in the direction of the stronger magnet. However, either configuration i.e., being buckled to the left or to the right, constitutes a stable equilibrium. The position of the beam in the center is an unstable equilibrium. A periodic lateral force was applied to the entire framework through a programmable motor.

We used strain gauges, attached near the base of the beam, to measure the displacement of the tip. The strain gauges were used to create a voltage differential which was then amplified and sent to the computer where it was plotted as a function of time. We used a of 10,000 Hz. We found an approximate linear correspondence between voltage and displacement of the beam: 1.4V corresponds to approximately .045 m. Thus, no scaling was required to measure the actual displacement.

Limitations of the apparatus: Our apparatus had the following limitations:

1. *Bend in the shim stock*: The metallic shim stock that we used had a natural bend in it which could not be completely removed through pre-processing. This bend caused the shim stock to favor a particular equilibrium.

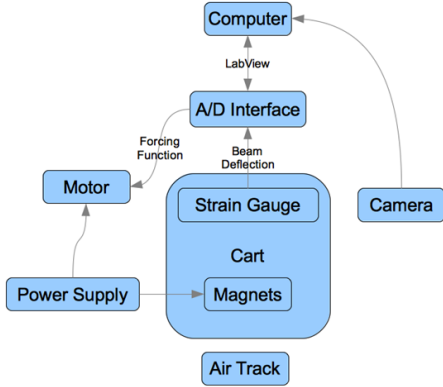


FIG. 2. Schematic diagram of apparatus

2. *Mechanical vibrations:* Although, we were able to reduce this problem by mounting the apparatus on cinderblocks yet minor vibrations owing to the movement of the motor still influence the beam.
3. *Heat:* Our motor heated up after prolonged use so some runs were prematurely terminated to avoid damage to the apparatus.
4. *Limited magnitude of forcing function:* We could not apply large force to the framework due to the limited distance the framework could move about its position.

B. Simulations

We also carried out computer simulations to study the Duffing oscillator. We estimated the values of α ; β ; and δ using our experi-

mental data. According to our data, we have fixed points at approximately $\sqrt{\pm \frac{\alpha}{\beta}} \approx \pm 0.7V$ (the strain gauges would shift over time, but this is the position once we normalize by subtracting the mean from the data). Writing $x(t) = -\sqrt{\frac{\alpha}{\beta}} + \phi(t)$, substituting this into the Duffing equation and ignoring the forcing term, we find that to first order in ϕ we have $\phi(t) = -\delta\ddot{\phi}(t) - 2\alpha\phi(t)$. This gives us damped simple harmonic motion with frequency $\sqrt{2\alpha(1 - \delta^2/8\alpha)}$. Solving in terms of δ gives us $\delta = \sqrt{8\alpha(1 - \omega_1^2/2\alpha)}$. From our experimental data we get an approximate value for ω_1 (based on the period of oscillation in the small amplitude case) and guess α such that $\omega_0 = \sqrt{2\alpha}$ is only slightly larger than ω_1 .

We set the parameters to the following values based on our data. From the dataset where the stock oscillated with low amplitude in the right well we find that $\omega_{1,left} = 2.0Hz$. We found chaotic behavior with $f = 6.272$ and $\alpha = 2.01$. For the left well we found that $\omega_{1,right} = 4.76Hz$ and $\alpha = 11.33$.

For our simulations we averaged the two values of ω_1 and thus used $\omega_{1,avg} = 3.38$ and $\alpha = 5.714$.

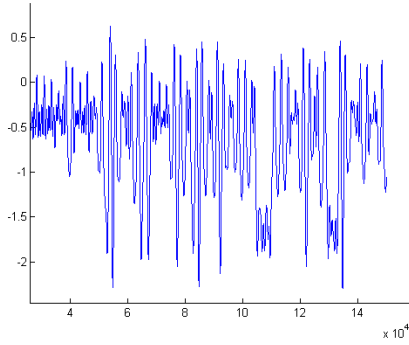


FIG. 3. Chaotic behavior for sinusoidal forcing:
Time series

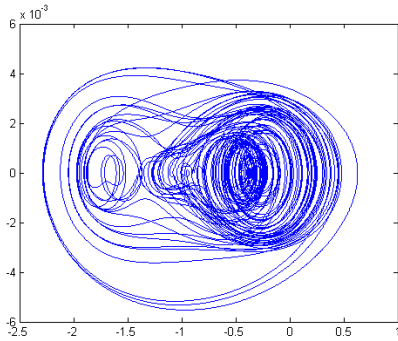


FIG. 4. Chaotic behavior for sinusoidal forcing:
Phase Plot

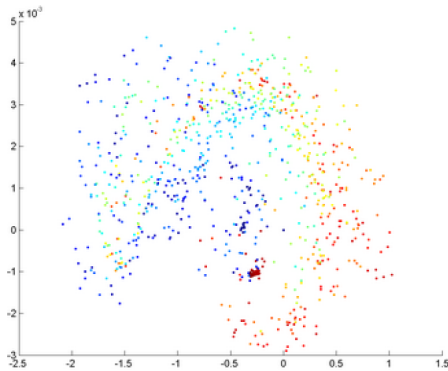


FIG. 5. Chaotic behavior for sinusoidal forcing:
Poincare section

V. RESULTS

A. Experimental data

We present results from one of our runs in which we observed chaotic behavior. The plot in figure 3 shows a time series plot of the voltage measurements collected during the run. One magnetic well is located at around $-0.4V$ (on the y -axis) and the other is at around $-1.8V$. One can see that the motions of the tip are highly irregular and indeed appear random. In order to clean the noise in the signal, we passed this data through a Butterworth filter. The processed data was then numerically differentiated. We plotted the smoothed signal versus its derivative to obtain the trajectory in phase space (x vs. \dot{x}) shown in figure 4. Finally, we obtained the Poincare section for the same data (figure 5) by plotting one point per oscillation of the motor. The motor was oscillating at 4 Hz and we were sampling at $10,000$ Hz so we plotted only the first of every $2,500$ data points. The points were then colored to indicate the sequence in which they were plotted.

B. Estimation of the largest Lyapunov Exponent

In order to reconstruct the attractors from time series we use the data shown in figure 3.

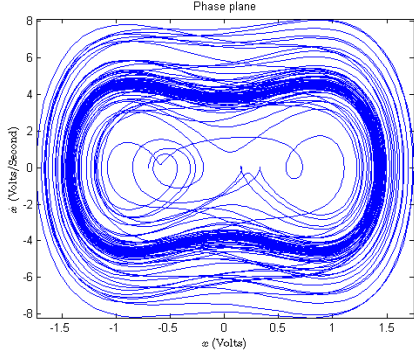


FIG. 6. Phase plot: Oscillations in right well with small f

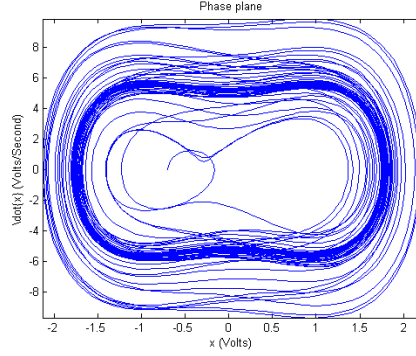


FIG. 8. Oscillations in left and right wells with small f

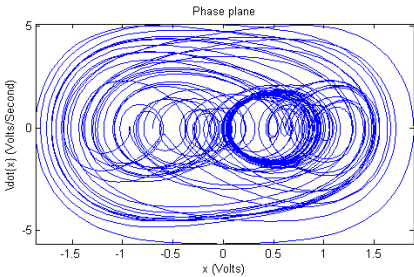


FIG. 7. Phase plot: Oscillations in left well with small f

We then estimated the largest Lyapunov exponent. We find the largest Lyapunov exponent to be .0196 - which is positive, as we would expect for a system exhibiting chaotic behavior.

C. Discussion

The phase plots of the simulations run with the parameters estimated earlier are shown in figures 6, 7, and 8. We notice several discrepancies between simulated and measured results. We find that only the simu-

lation using the right well parameters showed any significant chaotic behavior, and even in that case the chaotic transient ended fairly quickly in a limit cycle.

Additionally, the experimental results shown in figure 4 shows extreme asymmetry (the trajectories spending a disproportionately long time in the right well, which is apparently much larger than the left well). Whereas, the simulation plots are quite symmetric. We believe this asymmetry is due to the natural bend of the shim stock in the direction of the magnet corresponding to the right potential well. Additionally, as mentioned before, there is also a significant difference between the strength of the magnets, which contributes to this observed asymmetry.

VI. CONCLUSION

We carried out experiments with the Duffing oscillator in the presence of periodic lateral force. Our experiments did not produce chaotic behavior in majority of runs due to

certain backdraws of the apparatus. However, we found that chaotic behavior can even arise quickly in the presence of such asymmetries as present in our system. This also opens up directions for future work where we can analyze the Duffing oscillator in the presence of asymmetric wells.